

Supporting Information for

Chromis-1, A Ratiometric Fluorescent Probe Optimized for Two-Photon Microscopy Reveals Dynamic Changes in Labile Zn(II) in Differentiating Oligodendrocytes

Daisy Bourassa^{§‡}, Christopher M. Elitt^{†‡}, Adam M. McCallum[§], S. Sumalekshmy[§],
Reagan L. McRae[§], M. Thomas Morgan[§], Nisan Siegel[§], Joseph W. Perry^{*§},
Paul A. Rosenberg^{*†} and Christoph J. Fahrni^{*§}

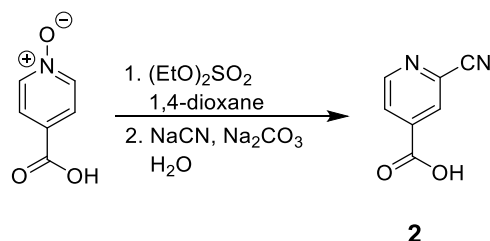
[§]School of Chemistry and Biochemistry and Petit Institute for Bioengineering and Bioscience, Georgia Institute of Technology, Atlanta, Georgia 30332, U.S.A.; [†]Department of Neurology and Program in Neuroscience, Children's Hospital and Harvard Medical School, Boston, Massachusetts 02115, U.S.A.

Table of Contents

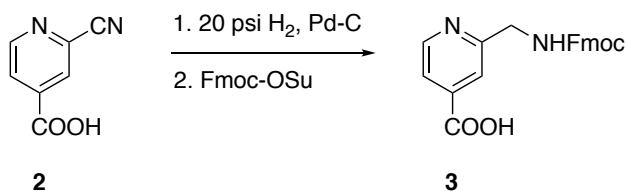
1. Synthetic Procedures	S2
2. ¹ H-NMR and ¹³ C-NMR Spectra	S9
3. Crystallographic Structural Determination	S16
4. Fluorescence Response Towards Divalent Metal Ions	S21
5. Ligand Competition Titrations	S22
6. Spectrophotometric Determination of Protonation Constants	S24
7. Ratiometric Data Analysis	S25
8. References	S28

1. Synthetic Procedures

Materials and Reagents. 2-Amino-4'-methoxyacetophenone (**4**) was synthesized according to a previously published procedure.¹ Fmoc-succinimidyl carbonate (Oakwood Chemicals), isonicotinic acid *N*-oxide (Alfa Aesar), 2,4-pyridine dicarboxylic acid (Alfa Aesar), and 2-bromo-4'-methoxyacetophenone (Alfa Aesar) were purchased commercially and used without further purification. NMR: ¹H NMR spectra were recorded at 400 MHz and referenced to an internal TMS standard (0 ppm) for all NMR solvents excluding D₂O, which was referenced to sodium 3-trimethylsilylpropionate-2,2,3,3-d₆ (0 ppm). ¹³C spectra were acquired at 100 MHz and referenced to the known chemical shift of the solvent peak (CDCl₃: 77.2 ppm; DMSO-d₆: 39.5 ppm; CD₃OD: 49.0 ppm; Acetone-d₆: 206.3, 29.8 ppm).

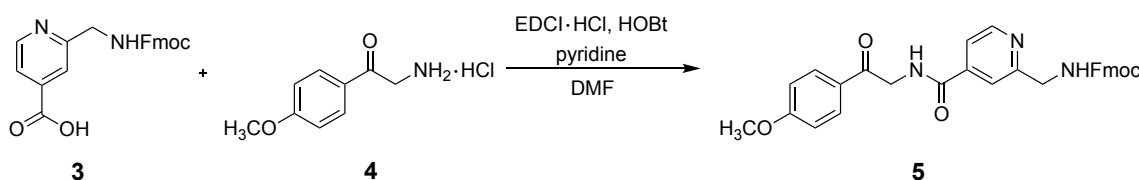


2-Cyanoisonicotinic acid (2). Isonicotinic acid *N*-oxide (87.7 mmol, 12.2 g), diethyl sulfate (1.2 eq., 105 mmol, 12.2 mL) and dioxane (15 mL) were added to a 100 mL round bottom flask containing a large stir bar. The flask was covered with a fritted adapter to minimize evaporation, and the mixture was stirred at 90°C overnight to produce a biphasic liquid. This was diluted with ice water (100 mL) and washed with an equal volume of ethyl acetate to remove tarry material and unreacted Et₂SO₄. The aqueous phase was neutralized with Na₂CO₃ (1.0 eq., 96.5 mmol, 9.3 g) under stirring, and NaCN (1.1 eq., 96.5 mmol, 4.73 g) was added. After 2 hours, the mixture was slowly acidified with concentrated HCl (2.1 eq., 184 mmol, 15 mL), and the product was collected by filtration and dried by suction overnight to give a red-orange powder, which was recrystallized from boiling acetonitrile-water gave the purified product as a light yellow solid. Yield: 10.67 g (82%). ¹H NMR (400 MHz, Acetone-d₆) δ 8.19 (dd, *J* = 5.0, 1.6 Hz, 1H), 8.35 (dd, *J* = 1.6, 0.9 Hz, 1H), 8.96 (dd, *J* = 5.0, 0.9 Hz, 1H). ¹³C NMR (100 MHz, Acetone-d₆) δ 117.7, 127.5, 128.7, 135.4, 140.5, 153.2, 164.8.

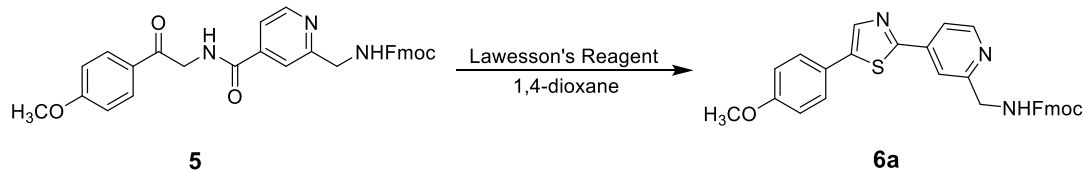


2-(((9H-Fluoren-9-yl)methoxy)carbonyl)amino)methylisonicotinic acid (3). A solution of 2-cyanoisonicotinic acid (**2**) (6.76 mmol, 1.0 g) in acetic acid (5 mL) was hydrogenated for 2 hours at 20 psi in the presence of Pd/C (5 mol %, 500 mg) as a catalyst. The reaction mixture was filtered through a pad of Celite and the solvent was removed under reduced pressure to give 950 mg (93%) of 2-(aminomethyl)isonicotinic acid. Without further purification, the isolated product (1.32 mmol, 200 mg) was dissolved in 10% aq. Na₂CO₃ (1.5

mL) and a solution of 9-fluorenylmethylsuccinimidyl carbonate (0.91 eq., 1.2 mmol, 405 mg) in 1,4-dioxane (1 mL) was added. After stirring the reaction mixture at room temperature for 12 hours, the solvent was evaporated and the residue was treated with 1 M aq. HCl (1.5 mL). The precipitated product was filtered off, washed with water and a small amount of methanol, and dried under vacuum to afford 420 mg (85%) of the Fmoc derivative **3** as a white solid. ^1H NMR (400 MHz, DMSO- d_6 , T = 373K) δ 4.22 (t, J = 6.9 Hz, 1H), 4.34 (d, J = 6.9 Hz, 2H), 4.39 (d, J = 6.1 Hz, 2H), 7.29 (t, J = 7.4 Hz, 2H), 7.38 (t, J = 7.4 Hz, 2H), 7.55 (s, br, 1H), 7.63-7.67 (m, 3H), 7.77 (s, 1H), 7.83 (d, J = 7.5 Hz, 2H), 8.66 (d, J = 5.0 Hz, 1H), 13.01 (s, broad, 1H). Note: Due to the presence of a dynamic conformer equilibrium, the room temperature ^1H NMR spectrum displayed an additional set of weak signals which merged with the main set upon heating to 100 °C. Furthermore, the dynamic exchange precluded the recording of a suitable ^{13}C NMR spectrum. MS (ESI) m/z 375 (100, $[\text{M}+\text{H}]^+$). HRMS (ESI) m/z calculated for $\text{C}_{22}\text{H}_{19}\text{N}_2\text{O}_4$ $[\text{M}+\text{H}]^+$ 375.1345, found 375.1356.



Fmoc-protected amide 5. A mixture of the Fmoc-protected amino acid **3** (9.62 mmol, 3.60 g), 2-amino-1-(4'-methoxyphenyl)ethanone hydrochloride **4** (1.1 eq., 10.6 mmol, 2.22 g), EDCI·HCl (1.5 eq., 14.4 mmol, 2.87 g), and 1-hydroxybenzotriazole (0.5 eq., 4.81 mmol, 675 mg) was stirred in DMF (12 mL) until it turned homogeneous (10 min). Pyridine (1.0 eq., 815 μL) was added, and the mixture was stirred overnight. The mixture was diluted sequentially with water (5 mL), methanol (60 mL) and water (20 mL) under rapid stirring. The resulting precipitate was collected by filtration, washed with water, dried under vacuum, and recrystallized from a solution in THF-acetonitrile by boiling until the temperature rose to the boiling point of pure CH_3CN . After cooling to room temperature, the product was collected by filtration and dried under high vacuum to afford a colorless crystalline powder. Yield: 4.59 g (8.80 mmol, 92%). ^1H NMR (400 MHz, DMSO- d_6 , T = 293 K) δ 3.86 (s, 3H), 4.26 (t, J = 5.0 Hz, 1H), 4.34 (d, J = 7.0 Hz, 2H), 4.39 (d, J = 6.0 Hz, 2H), 4.78 (d, J = 5.6 Hz, 2H), 7.09 (d, J = 8.8 Hz, 2H), 7.33 (t, J = 7.5 Hz, 2H), 7.41 (t, J = 7.4 Hz, 2H), 7.70-7.76 (m, 4H), 7.90 (d, J = 7.5 Hz, 2H), 8.01-8.05 (m, 3H), 8.69 (d, J = 5.1 Hz, 1H), 9.09 (t, broad, J = 5.6 Hz, NH). ^{13}C NMR (100 MHz, DMSO- d_6) δ 45.8, 46.1, 46.7, 55.6, 65.7, 114.1, 118.5, 119.5, 120.1, 125.3, 127.1, 127.7, 127.8, 130.3, 140.7, 141.7, 143.9, 149.6, 156.5, 160.0, 163.5, 165.2, 193.1. MS (ESI) m/z 522 (100, $[\text{M}+\text{H}]^+$), 177 (18); HRMS (ESI) m/z calculated for $\text{C}_{31}\text{H}_{28}\text{N}_3\text{O}_5$ $[\text{M}+\text{H}]^+$ 522.2029, found 522.2066.

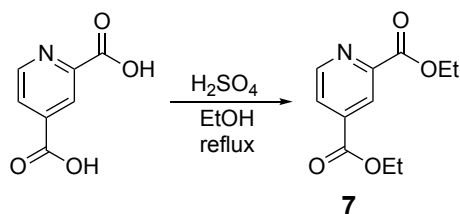


Fmoc-protected thiazole 6a. Amide **5** (2.01 mmol, 1.046 g) and Lawesson's reagent (1.2 eq., 2.41 mmol, 973 mg) were added to a 25 mL round bottom flask equipped with a magnetic stir bar. The flask was clamped above a 120°C oil bath and fitted with a reflux condenser, which was topped with a T-shaped adapter leading to an argon supply and bubbler. The joint between the condenser and flask was pulled apart to leave a gap of a few mm, and the system was flushed with argon. Anhydrous 1,4-dioxane (4 mL) was added from a syringe through the gap in the joint. The joint was quickly seated, and the flask was lowered into the oil bath. After 30 minutes, the reaction was complete by TLC (5:1 CH₂Cl₂-MTBE). Water (~0.5 mL) was added while stirring, and the mixture was allowed to cool to room temperature. The resulting orange slurry was dissolved in CH₂Cl₂ (12 mL) and stirred with 5% aqueous NaOH (6 mL, 4 equiv.) for 20 min. The resulting yellow emulsion was partitioned between water (50 mL) and CH₂Cl₂ (50 mL) and the organic layer was collected. The aqueous layer was extracted with CH₂Cl₂ (10 mL) and the combined organic layers were dried with MgSO₄, diluted with MTBE (10 mL), and filtered through a bed of sand (~4 cm) on top of silica gel (~6 cm). The filter was washed with 3:1 CH₂Cl₂-MTBE until the effluent was no longer yellow, and the combined filtrate and washings were concentrated to dryness. The residue was recrystallized from ethyl acetate/2,2,4-trimethylpentane to give pure **6a** as light yellow fibrous crystals. Yield: 891 mg (1.72 mmol, 86%). ¹H NMR (400 MHz, CDCl₃) δ 3.86 (s, 3H), 4.27 (t, *J* = 7.1 Hz, 1H), 4.44 (d, *J* = 7.1 Hz, 2H), 4.61 (d, *J* = 5.4 Hz, 2H), 5.96 (t, broad, *J* = 4.9 Hz, 1H), 6.96 (d, *J* = 8.8 Hz, 2H), 7.31 (t, *J* = 7.4 Hz, 2H), 7.39 (t, *J* = 7.4 Hz, 2H), 7.53 (d, *J* = 8.8 Hz, 2H), 7.64 (d, *J* = 7.4 Hz, 2H), 7.71 (dd, *J* = 5.2, 1.4 Hz, 1H), 7.76 (d, *J* = 7.5 Hz, 2H), 7.79 (s, br, 1H), 7.99 (s, 1H), 8.64 (d, *J* = 5.1 Hz, 1H). ¹³C NMR (100 MHz, CDCl₃) δ 46.0, 47.2, 55.4, 67.0, 114.7, 118.1, 118.9, 119.9, 123.3, 125.1, 127.0, 127.7, 128.2, 139.0, 141.3, 141.4, 141.7, 144.0, 149.9, 156.5, 157.9, 160.3, 162.5. MS (ESI) *m/z* 520 (100, [M+H]⁺); HRMS (ESI) *m/z* calculated for C₃₁H₂₆N₃O₃S [M+H]⁺ 520.1695, found 520.1719.

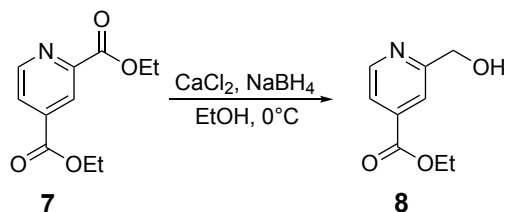


Amine 6b. A 50-mL round bottom flask was charged with **6a** (2.02 mmol, 1.049 g), crushed cesium carbonate (2 eq., 4.04 mmol, 1.315 g) and DMSO (15 mL). Ethanethiol (2 eq., 4.04 mmol, 291 μL) was added drop-wise to the stirred mixture. After 1.5 hours, the reaction was complete by TLC (neat EtOAc). The mixture was transferred to a 250-mL Erlenmeyer flask, partitioned between diH₂O (50 mL) and toluene (25 mL), and heated gently until two homogeneous liquid phases could be separated. The mixture was acidified with 1 M aq. HCl

(1 eq., ~ 2 mL), and the orange aqueous layer was collected, washed with toluene to remove non-basic byproducts, and then made basic (pH ~ 9) by the addition of 5% aq. NaOH. The product was extracted with toluene (2 x 25 mL), and the combined extracts were dried over MgSO₄, filtered, and concentrated to afford **6b** as a pure, pale yellow solid. Yield 454 mg (1.53 mmol, 76%). ¹H NMR (400 MHz, CDCl₃) δ 3.87 (s, 3H), 4.07 (s, 2H), 6.97 (d, *J* = 8.9 Hz, 2H), 7.55 (d, *J* = 8.9 Hz, 2H), 7.68 (dd, *J* = 5.2, 1.7 Hz, 1H), 7.82-7.83 (m, 1H), 8.00 (s, 1H) 8.65 (dd, *J* = 5.2, 0.8 Hz, 1H). ¹³C NMR (100 MHz, CDCl₃) δ 47.7, 55.4, 114.6, 117.4, 118.2, 123.3, 128.1, 138.8, 140.9, 141.3, 150.1, 160.1, 162.9, 163.0. MS (EI) *m/z* 297 (100, [M]⁺), 268 (45), 149 (10); HRMS (EI) *m/z* calculated for C₁₆H₁₅N₃OS [M]⁺ 297.0936, found 297.0921.

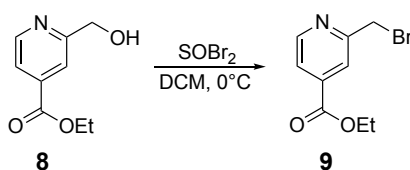


Ethyl 2,4-pyridinedicarboxylate (7). Adapted from a previously published procedure.² 2,4-pyridinedicarboxylic acid (1 eq., 29.9 mmol, 5.0 g) was suspended in absolute ethanol (50 mL), and concentrated H₂SO₄ (1.5 eq., 47.1 mmol, 2.62 mL) was added drop-wise to the stirred mixture. After refluxing overnight, the EtOH was removed under reduced pressure, and the resulting oily residue was partitioned between CHCl₃ (50 mL) and saturated Na₂CO₃ (20 mL). The organic layer was removed, and the aqueous layer was extracted with CHCl₃ (2 x 50 mL). The combined organic layers were dried over anhydrous MgSO₄, filtered, and concentrated to a yellow oil. The yellow oil was then taken up in boiling cyclohexane and crystallized while cooling to room temperature under constant stirring. The product was collected by suction filtration, washed with cyclohexane, and dried under vacuum to afford **7** as a white crystalline solid. Yield 5.52 g (24.7 mmol, 83%). ¹H NMR (400 MHz, CDCl₃) δ 1.44 (t, *J* = 6.5 Hz, 3H), 1.48 (t, *J* = 6.5 Hz, 3H), 4.46 (q, *J* = 7.1 Hz, 2H), 4.53 (q, *J* = 7.1 Hz, 2H), 8.05 (dd, *J* = 4.9, 1.6 Hz, 1H), 8.65 (dd, *J* = 1.6, 0.8 Hz, 1H), 8.92 (dd, *J* = 4.9, 0.9 Hz, 1H). ¹³C NMR (100 MHz, CDCl₃) δ 14.3, 14.4, 62.3, 62.4, 124.4, 126.1, 139.2, 149.3, 150.8, 164.4, 164.7. MS (EI) *m/z* 223 (4, [M]⁺), 179 (35), 178 (40), 152 (33), 151 (100), 150 (45), 123 (30), 78 (18), 77 (21). HRMS (EI) *m/z* calculated for C₁₁H₁₃NO₄ [M]⁺ 223.0845, found 223.0842.

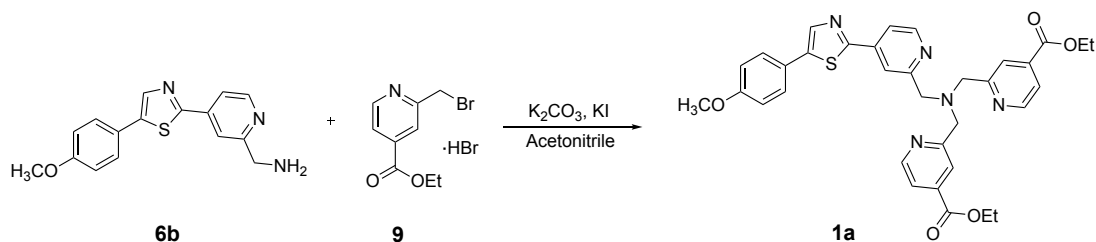


Ethyl 2-(hydroxymethyl)isonicotinate (8). Adapted from a previously published procedure.² To a solution of ethyl 2,4-pyridinedicarboxylate (**7**, 1 eq., 24.6 mmol, 5.50 g) in EtOH (50 mL) at 0°C was added crushed anhydrous CaCl₂ (1 eq., 24.6 mmol, 2.73 g). While stirring under argon, NaBH₄ (1 eq., 24.6 mmol, 932 mg) was added slowly to the slightly

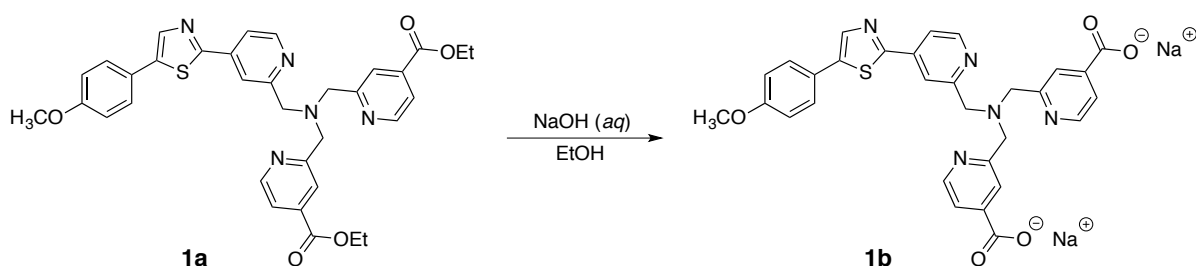
opaque mixture, and upon the complete addition of NaBH₄, the mixture turned a bright pink color. The reaction mixture was stirred for 2.5 hours at 0 °C until TLC (3:7 EtOAc:hexanes) confirmed that the reaction was complete. The reaction was quenched with the addition of 6 N HCl (1 eq., 4.1 mL), the white precipitate that formed was filtered off, and filtrate was concentrated under reduced pressure to remove most of the EtOH. The product was portioned between dichloromethane (50 mL) and saturated Na₂CO₃ to neutralize the HCl, followed by the addition of 1 M aq. disodium citrate to dissolve the inorganic salts that precipitated upon basification of the aqueous phase. The aqueous phase was extracted with dichloromethane (2 x 50 mL), and the combined organic layers were dried over anhydrous Na₂SO₄, filtered, and concentrated to a colorless oil. Residual CH₂Cl₂ was removed azeotropically with hexanes under reduced pressure, and the compound was dried under high vacuum to afford **8** as colorless crystals. Yield: 4.47 g (24.7 mmol, 72%). ¹H NMR (400 MHz, CDCl₃) δ 1.48 (t, *J* = 7.2 Hz, 3H), 4.12 (s, broad, 1H), 4.42 (q, *J* = 7.2 Hz, 2H), 4.85, (s, 2H), 7.77 (ddt, *J* = 5.1, 1.6, 0.7 Hz, 1H), 7.87 (ddt, *J* = 1.6, 0.8, 0.7 Hz, 1H), 8.69 (dd, *J* = 5.1, 0.9 Hz, 1H). ¹³C NMR (100 MHz, CDCl₃) δ 14.3, 62.0, 64.4, 120.0, 121.6, 138.5, 149.4, 160.9, 165.1. MS (EI) *m/z* 182 (20), 181 (85, [M]⁺), 180 (100), 178 (40), 153 (45), 152 (95), 151 (34), 136 (54), 124 (58), 123 (29), 108 (20), 78 (44), 51 (44). HRMS (EI) *m/z* calculated for C₉H₁₁NO₃ [M]⁺ 181.0749, found 181.0736.



Ethyl 2-(bromomethyl)isonicotinate (9). A 25 mL round bottom flask equipped with a stir bar was charged with **8** (1 eq., 5.52 mmol, 1.0 g), fitted with a rubber septum, evacuated under high vacuum, and backfilled with argon. Anhydrous dichloromethane (10 mL) was added via an argon-filled syringe, and the flask was cooled to 0 °C in an ice bath. Under stirring, thionyl bromide (SOBr₂, 3 eq., 16.6 mmol, 1.28 mL) was added via an argon-purged syringe, and the solution was allowed to stir for 1.5 hours. Unreacted thionyl bromide was quenched by the addition of EtOH (20 mL) followed by stirring for an additional 20 min. After concentrating the solution under reduced pressure, the residue was redissolved in a minimal amount of EtOH, and then diluted slowly with methyl *tert*-butyl ether (MTBE) until the solution became cloudy. The compound was then crystallized from boiling EtOH/MTBE to afford hydrobromide **9** as a white crystalline solid. Yield 1.46 g (4.5 mmol, 81%). ¹H NMR (400 MHz, CDCl₃) δ 1.48 (t, *J* = 7.2 Hz, 3H), 4.54 (q, *J* = 7.2 Hz, 2H), 5.19 (s, 2H), 8.48 (dd, *J* = 5.9, 1.5 Hz, 1H), 8.55 (s, 1H), 9.14 (d, *J* = 5.9 Hz, 1H). ¹³C HMR (100 MHz, CDCl₃) δ 14.1, 24.1, 63.9, 125.9, 128.0, 142.6, 146.3, 153.4, 161.4. Note: ¹H and ¹³C NMRs were acquired of the hydrobromide salt of **9** in CDCl₃ because of stability issues with the free base. MS (EI) *m/z* 244 (20), 243 (20, [M]⁺), 165 (19), 164 (100), 120 (33), 82 (18), 80 (20), 64 (19). HRMS (EI) *m/z* calculated for C₉H₁₀NO₂Br [M]⁺ 242.9895, found 242.9889.



Chromis-1 ester (1a). A mixture of **6b** (0.67 mmol, 200 mg), ethyl 2-(bromomethyl)isonicotinate hydrobromide (**9**, 2.5 eq., 1.68 mmol, 459 mg), crushed anhydrous potassium carbonate (2.5 eq., 1.68 mmol, 232 mg), and potassium iodide (2.5 eq., 1.68 mmol, 280 mg) in acetonitrile (12 mL) was stirred at room temperature under an argon atmosphere for 12 hours. The reaction mixture was diluted subsequently with EtOAc (10 mL) followed by diH₂O (10 mL). The organic layer was separated, dried over anhydrous Na₂SO₄, and evaporated under reduced pressure. The resulting residue was purified by column chromatography (silica gel, 1:1 dichloromethane/acetone). The oily column product was crystallized by redissolving in a minimal amount of EtOAc and slowly diluting with MTBE until cloudy, after which the mixture was heated to boiling to become homogeneous and concentrated until crystallization began to initialize. The crystals were isolated by suction filtration, washed with MTBE and dried under vacuum to give diester **1a** as a light yellow solid. Yield 320 mg (0.513 mmol, 76%). ¹H NMR (400 MHz, CDCl₃) δ 1.37 (t, *J* = 7.2 Hz, 6H), 3.88 (s, 3H), 4.03 (s, 2H), 4.07 (s, 4H), 4.37 (q, *J* = 7.1 Hz, 4H), 6.98 (d, *J* = 8.9 Hz, 2H), 7.59 (d, *J* = 8.9 Hz, 2H), 7.69-7.72 (m, 3H), 7.99 (s, 1H), 8.12-8.14 (m, 3H), 8.61 (dd, *J* = 5.2, 0.7 Hz, 1H), 8.69 (dd, *J* = 5.0, 0.8 Hz, 2H). ¹³C NMR (100 MHz, CDCl₃) δ 14.1, 55.4, 60.08, 60.14, 61.6, 114.5, 118.1, 119.6, 121.3, 122.4, 123.4, 128.1, 138.2, 138.8, 141.0, 141.3, 149.76, 149.78, 160.10, 160.14, 160.2, 163.2, 165.1. MS (EI) *m/z* 623 (5, [M]⁺), 459 (100), 342 (77), 282 (48), 137 (10). HRMS (EI) *m/z* calculated for C₃₄H₃₃N₅O₅S [M]⁺ 623.2202, found 623.2193.



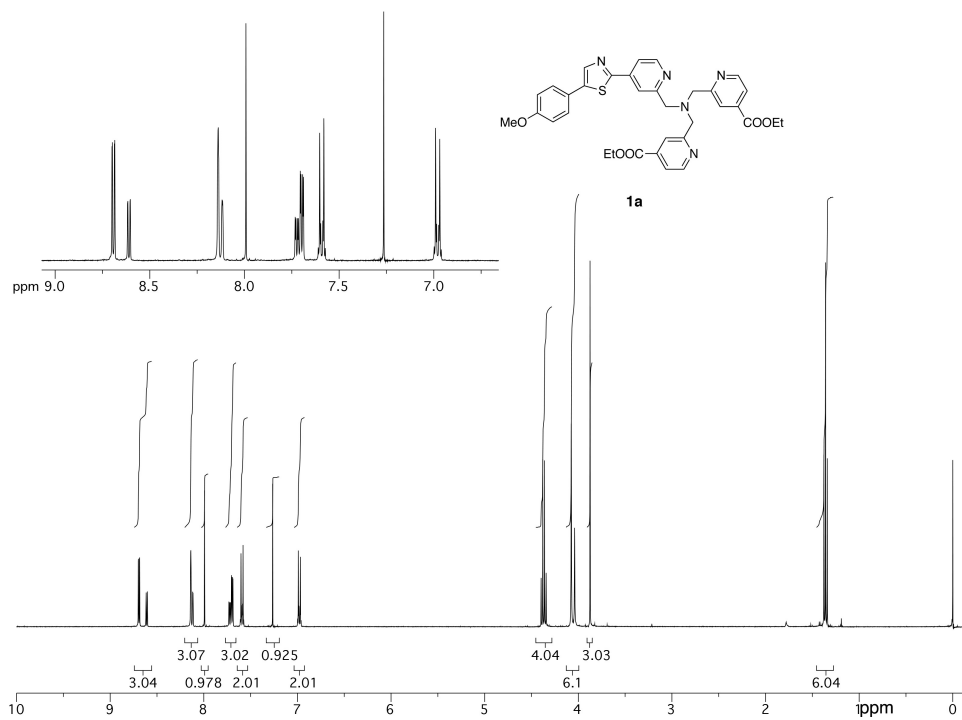
Chromis-1 acid (1b). Sodium hydroxide (2.5 eq., 0.40 mmol, 80.4 μL of a 20 % (w/v) aqueous solution) was added to a stirred solution of **1a** (1 eq., 0.16 mmol, 100 mg) in EtOH (4 mL), and the resulting mixture was refluxed under stirring for 2 hours. After cooling to room temperature, the product was filtered and dried under reduced pressure to afford 90 mg (0.15 mmol, 92% yield) of **1b** as pale yellow crystals. ¹H NMR (400 MHz, CD₃OD): δ 3.85 (s, 3H), 3.95 (s, 2H), 4.00 (s, 4H), 7.03 (d, *J* = 8.9 Hz, 2H), 7.65-7.68 (m, 4H), 7.75 (dd, *J* = 5.3, 1.8 Hz, 1H), 7.97-8.0 (m, 3H), 8.10 (s, 1H), 8.53 (d, *J* = 5.1 Hz, 3H). ¹³C NMR (100 MHz, CD₃OD): δ 54.4, 59.3, 60.0, 114.3, 118.1, 119.7, 121.8, 123.0, 123.1, 127.9, 138.5, 141.2, 142.1, 147.0,

148.8, 149.5, 158.3, 160.0, 160.5, 162.6, 171.1. HRMS (ESI) m/z calculated for $C_{30}H_{24}N_5Na_2O_5S$ $[M+H]^+$ 612.1294, found 612.1287.

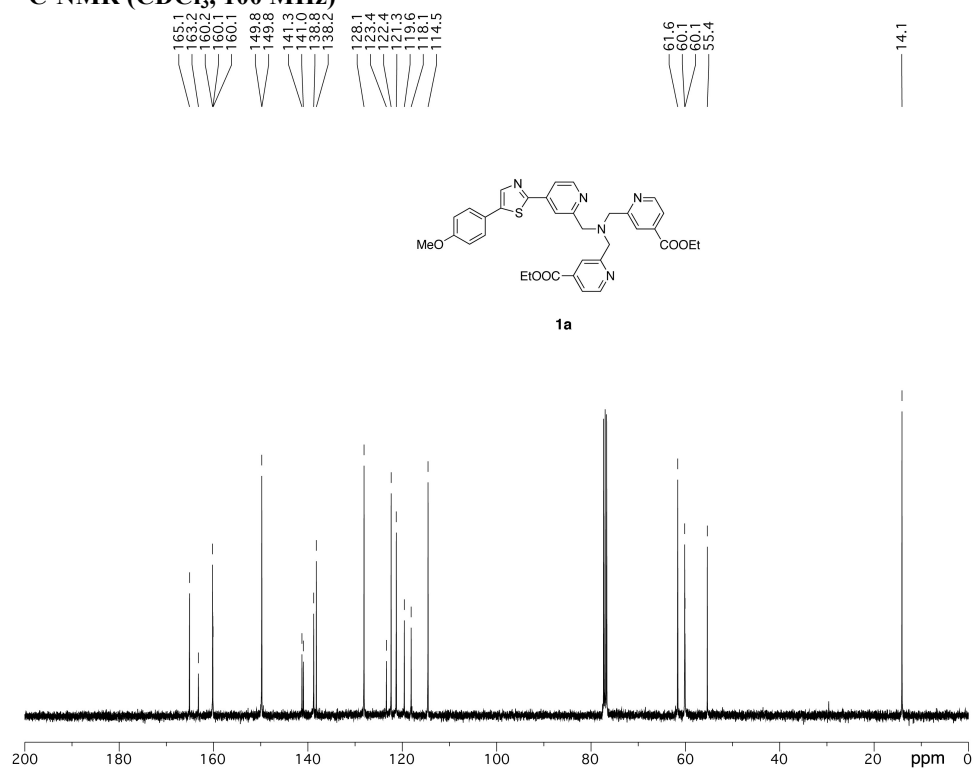
Chromis-1-Zn(II) Complex. Chromis-1 acid (**1b**, 20 mg) was reacted with a stoichiometric quantity of $ZnCl_2$ in HPLC-grade MeOH (2 mL). The precipitated Zn(II) complex was then redissolved in boiling MeOH and recrystallized from a MeOH-EtOH mixture to afford bright yellow crystals, which were filtered through a glass frit and washed with cold MeOH and EtOH and dried under vacuum. The crystals were carefully redissolved in a minimal amount of DMF:H₂O, and the solution was supplemented with crushed anhydrous $CaCl_2$ (0.5 eq., 1.8 mg). Slow evaporation of the corresponding solution afforded X-ray-quality crystals of the Zn(II) complex with formula $[Zn(II)Cl(chromis-1)]_2 \cdot Ca(DMF)(H_2O)_6$.

2. ^1H and ^{13}C NMR Spectra

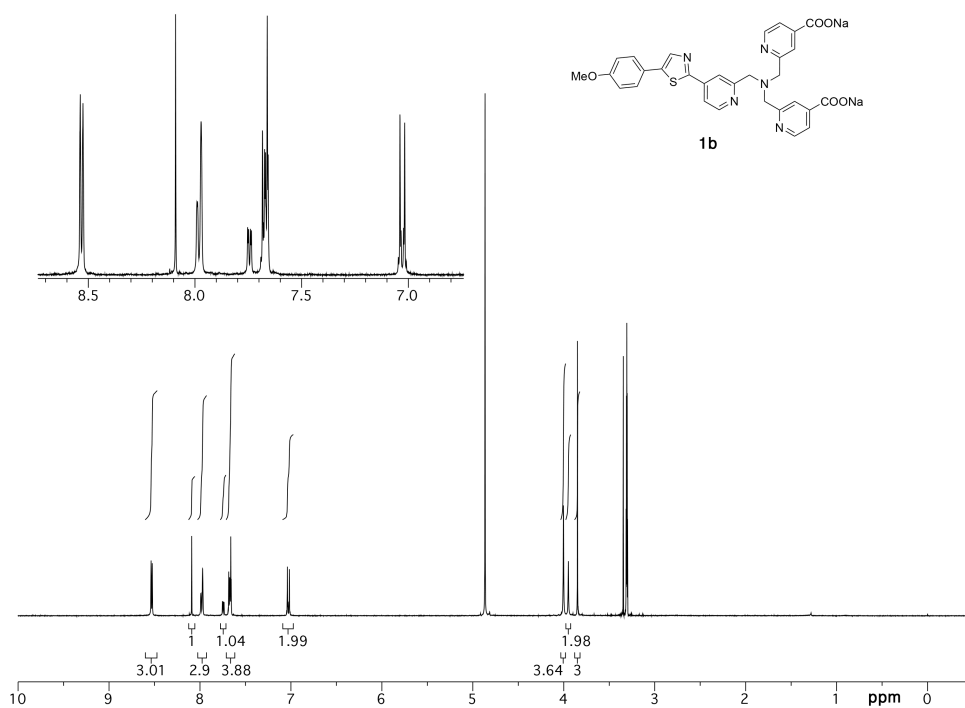
^1H -NMR (CDCl_3 , 400 MHz)



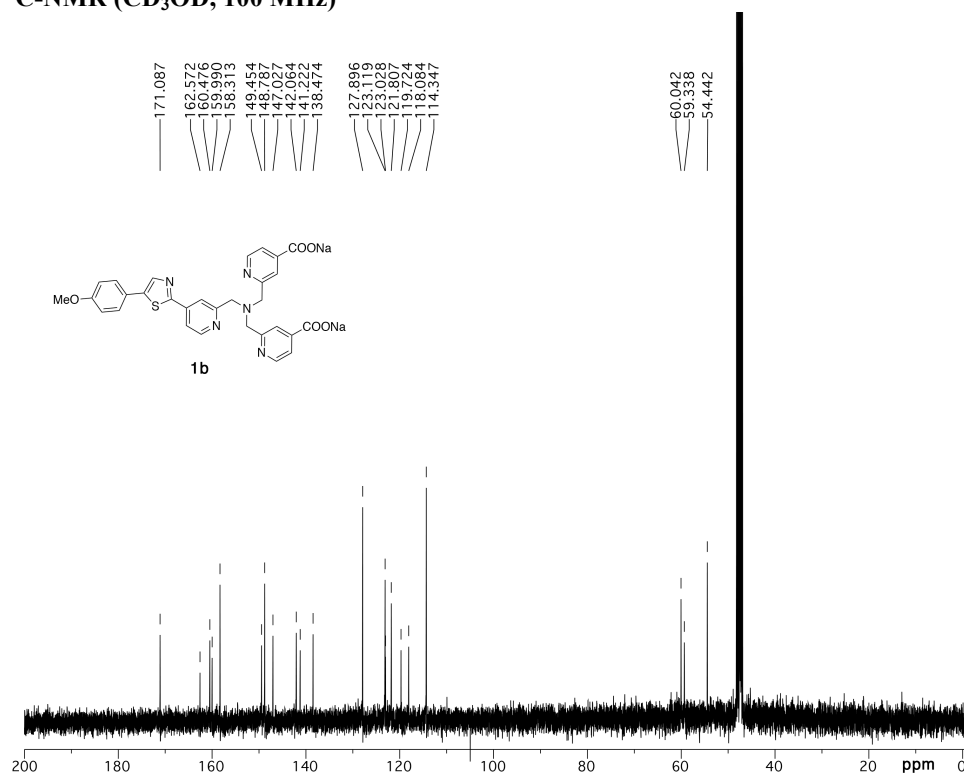
^{13}C -NMR (CDCl_3 , 100 MHz)



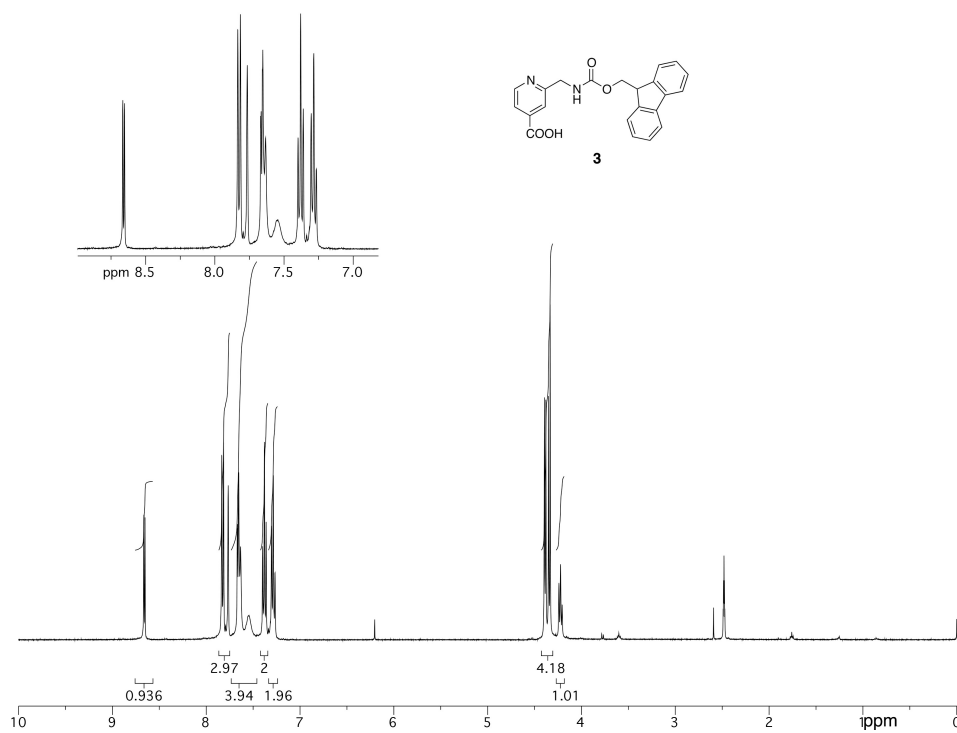
¹H-NMR (CD₃OD, 400 MHz)



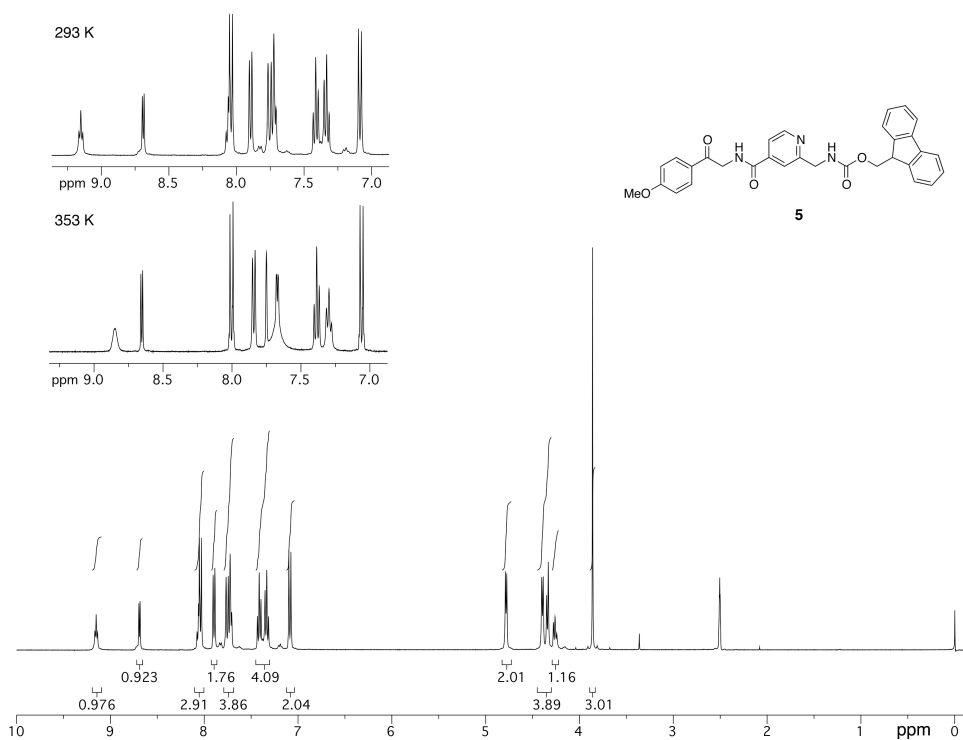
¹³C-NMR (CD₃OD, 100 MHz)



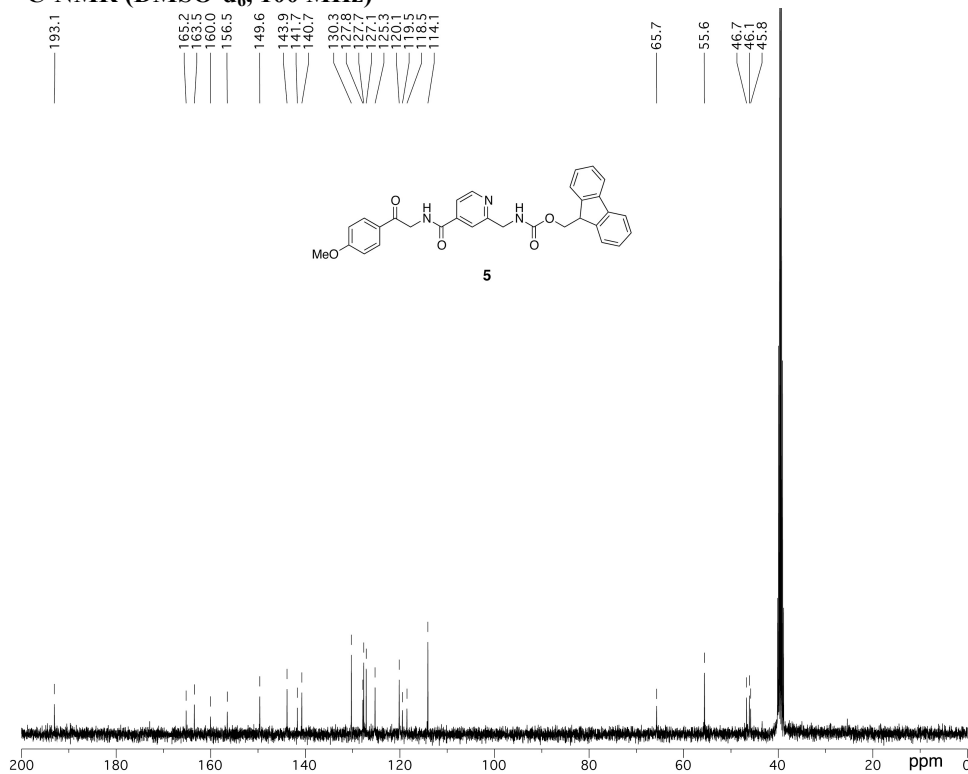
¹H-NMR (DMSO-d₆, 400 MHz, T = 373 K)



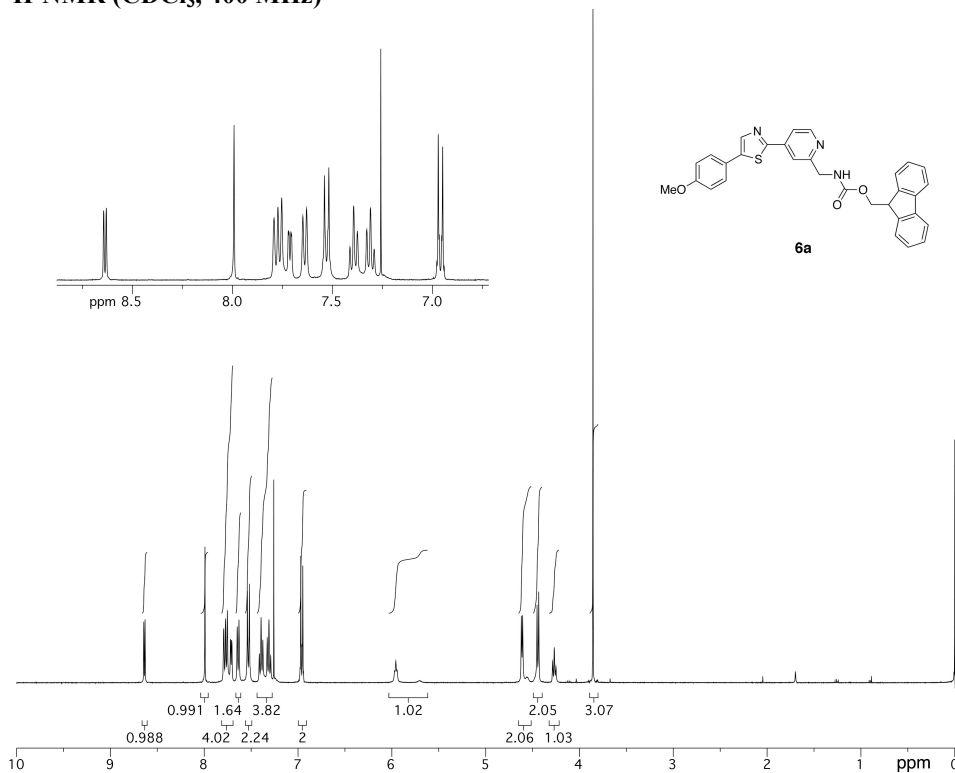
¹H-NMR (DMSO-d₆, 400 MHz, T = 293 K)



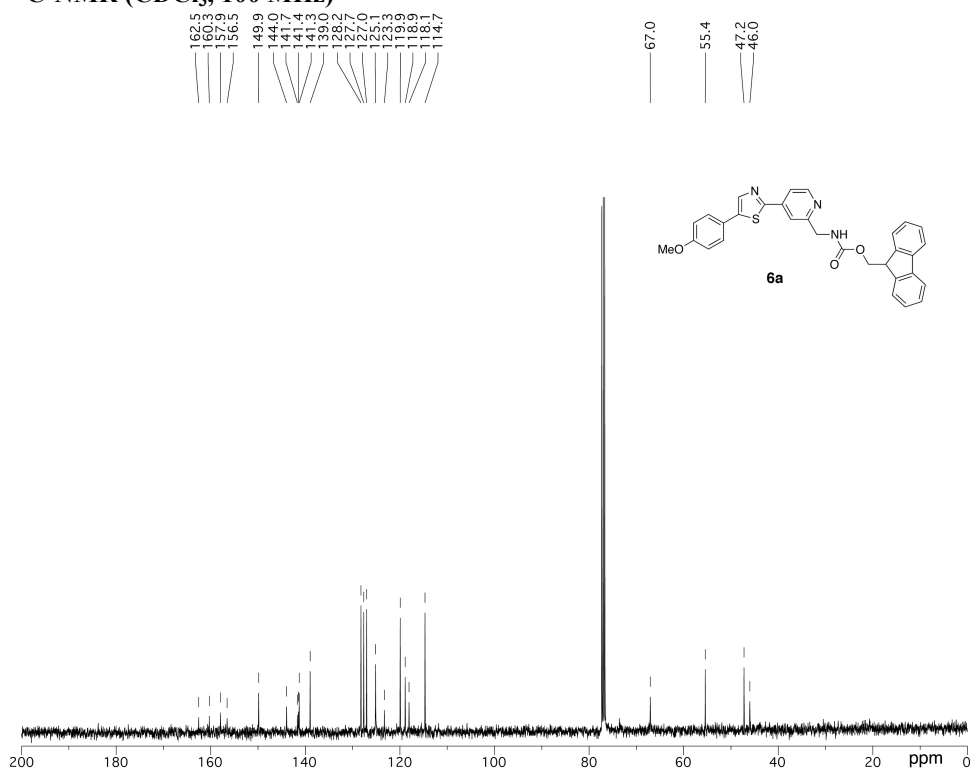
¹³C-NMR (DMSO-d₆, 100 MHz)



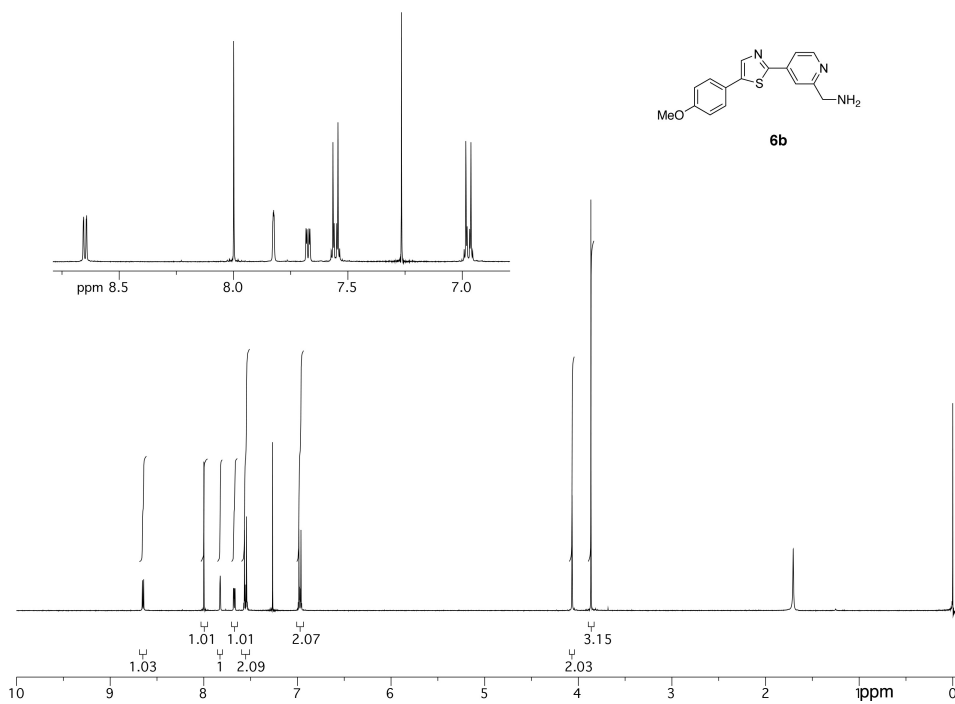
¹H-NMR (CDCl₃, 400 MHz)



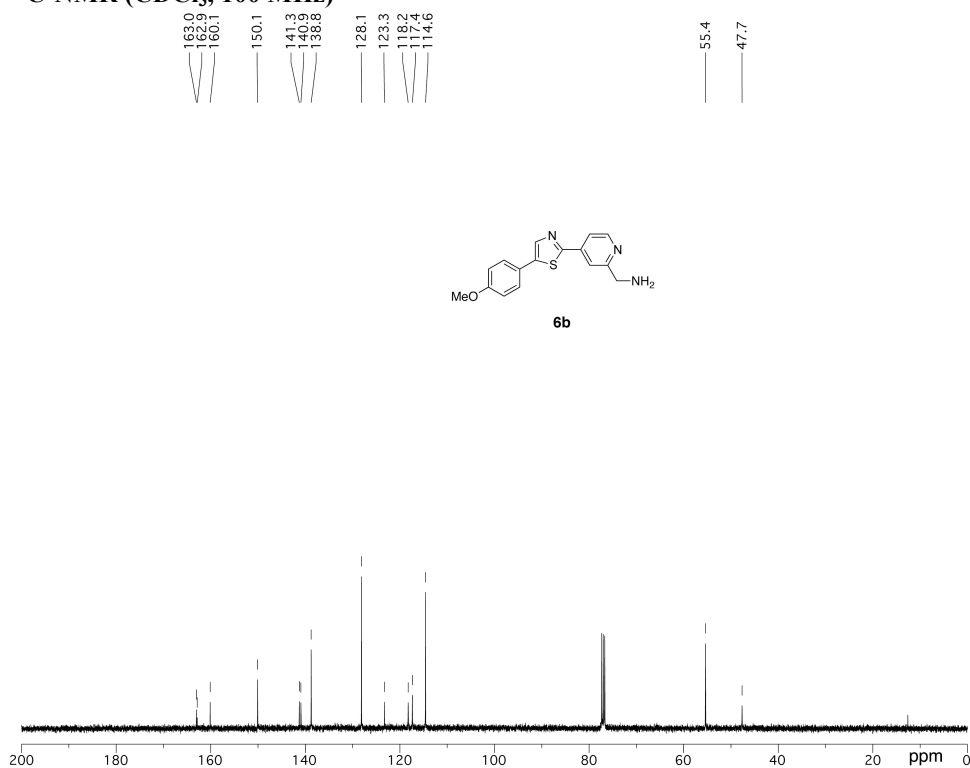
¹³C-NMR (CDCl₃, 100 MHz)



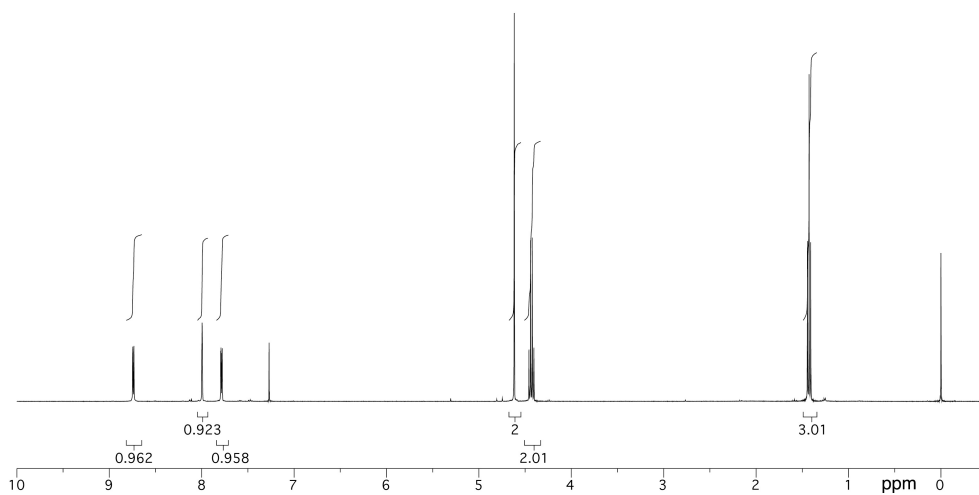
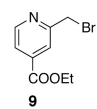
¹H-NMR (CDCl₃, 400 MHz)



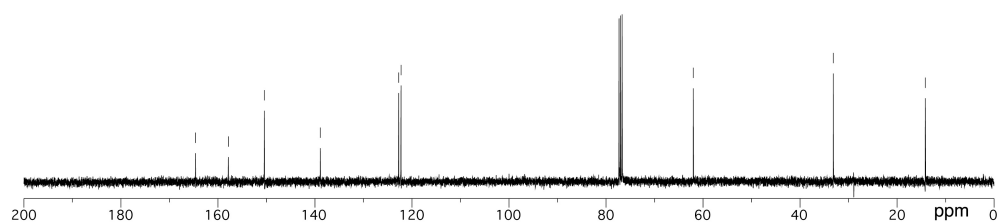
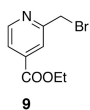
¹³C-NMR (CDCl₃, 100 MHz)



¹H-NMR (CDCl₃, 400 MHz)



¹³C-NMR (CDCl₃, 100 MHz)



3. Crystallographic Structural Determination

Table S1: Crystal data and structure refinement for the Zn(II) complex of ligand **1b** [Zn(II)Cl(chromis-1)]₂Ca(DMF)(H₂O)₆

Empirical formula	C ₆₃ H ₆₅ CaCl ₂ N ₁₁ O ₁₇ S ₂ Zn ₂	
Formula weight	1554.16	
Temperature	100(2)	
Wavelength	MoK α (λ = 0.71073)	
Crystal system	Triclinic	
Space group	P-1	
Unit cell dimensions	a = 11.8106(6) Å	α = 79.625(4)°
	b = 13.3625(6) Å	β = 81.802(4)°
	c = 22.2111(11) Å	γ = 77.504(4)°
Volume	3346.7(3) Å ³	
Z	2	
Density (calculated)	1.542 g/cm ³	
Absorption coefficient	1.014 mm ⁻¹	
F(000)	1604.0	
Crystal size	0.218 × 0.093 × 0.028 mm	
Theta range for data collection	1.580 to 24.712°	
Index ranges	-13 ≤ h ≤ 13, -15 ≤ k ≤ 15, -26 ≤ l ≤ 26	
Reflections collected	27927	
Independent reflections	11181 [R _{int} = 0.1247, R _{sigma} = 0.1227]	
Refinement method	Full-matrix least-squares on F ²	
Data / restraints / parameters	11181/836/911	
Goodness-of-fit on F ²	1.063	
Final R indices [I > 2σ(I)]	R ₁ = 0.0899, wR ₂ = 0.1820	
R indices (all data)	R ₁ = 0.1502, wR ₂ = 0.2195	
Largest diff. peak and hole	1.552/-0.762 e·Å ⁻³	

Table S2: Selected bond lengths and bond angles for the two conformers of the Zn(II) complex of ligand **1b** [Zn(II)Cl(chromis-1)]₂Ca(DMF)(H₂O)₆ contained within the same unit cell.

Zn1-Cl1	2.266(2)	2.252(2)
Zn1-N1	2.101(7)	2.098(7)
Zn1-N2	2.088(7)	2.116(7)
Zn1-N3	2.097(7)	2.095(7)
Zn1-N4	2.254(7)	2.244(7)
N1-Zn1-Cl1	98.9(2)	103.6(2)
N1-Zn1-N2	117.8(3)	117.3(3)
N1-Zn1-N3	115.0(3)	114.6(3)
N1-Zn1-N4	77.0(3)	76.4(3)
N2-Zn1-Cl1	104.8(2)	101.9(2)
N2-Zn1-N3	112.9(3)	112.2(3)
N2-Zn1-N4	77.3(3)	76.1(3)
N3-Zn1-Cl1	104.7(2)	105.1(2)
N3-Zn1-N4	77.4(3)	77.0(3)
N4-Zn1-Cl1	175.69(2)	177.66(2)

Table S3: Atomic coordinates ($\times 10^4$) and equivalent isotropic displacement parameters ($\text{\AA}^2 \times 10^3$) for the unit cell of the Zn(II) complex of ligand **1b** $[\text{Zn(II)Cl(chromis-1)}]_2\text{-Ca(DMF)(H}_2\text{O)}_6$. $U(\text{eq})$ is defined as one third of the trace of the orthogonalized U^{ij} tensor.

Atom Label	x	y	z	U(eq)
Zn1	7283.9(9)	8179.9(8)	7512.0(5)	15.4(2)
Cl1	8452(2)	8238.4(17)	8225(1)	20.9(5)
S1	3496(2)	4311.5(18)	8531.2(10)	19.1(5)
O2	3693(6)	13138(5)	7350(3)	22.9(14)
O4	11592(6)	5793(5)	5424(3)	25.6(12)
O1	-177(6)	993(5)	9318(3)	23.9(13)
N2	6382(6)	9704(5)	7305(3)	16.1(12)
N5	4458(7)	4373(6)	9490(3)	18.4(14)
N1	6346(6)	7080(5)	8022(3)	16.4(11)
O5	10219(6)	6392(7)	4783(3)	44(2)
N3	8434(6)	7671(5)	6769(3)	16.6(11)
N4	6062(6)	8041(5)	6852(3)	16.0(8)
C3	5074(7)	5556(6)	8604(4)	15.0(12)
C25	7980(8)	7282(7)	6358(4)	17.4(14)
C16	5035(8)	7738(7)	7228(4)	16.9(12)
C8	3118(8)	3523(7)	9202(4)	18.9(14)
C18	5722(8)	9903(7)	6839(4)	16.0(12)
C10	2205(8)	2337(7)	8768(4)	20.1(16)
C9	2280(8)	2845(7)	9249(4)	19.1(14)
C27	9848(8)	6855(7)	5787(4)	18.5(14)
C29	9590(8)	7685(7)	6679(4)	19.1(13)
C1	5382(7)	6962(6)	7792(4)	14.4(13)
C4	6031(8)	5714(7)	8841(4)	18.0(16)
C14	1495(8)	2728(7)	9784(4)	20.7(16)
C6	4403(8)	4777(7)	8910(4)	18.2(12)
C17	5802(8)	9062(6)	6464(4)	15.4(12)
C7	3703(8)	3691(7)	9649(4)	21.9(17)
C22	6355(8)	10444(7)	7642(4)	20.3(18)
C21	5626(8)	11431(7)	7537(4)	18.5(17)
C23	4147(8)	12682(7)	6906(4)	18.6(15)
C26	8661(8)	6896(7)	5857(4)	19.3(16)
C13	666(8)	2109(7)	9826(4)	20.2(16)
C12	610(8)	1606(7)	9328(4)	19.5(15)
C20	4964(8)	11645(7)	7046(4)	17.0(15)
C2	4756(8)	6211(7)	8057(4)	17.9(13)
C11	1404(8)	1708(7)	8807(4)	18.3(15)
C5	6664(8)	6456(6)	8548(4)	15.5(14)
C19	5023(8)	10872(7)	6689(4)	15.8(13)
C28	10313(8)	7281(7)	6196(4)	20.2(16)

C24	6707(7)	7221(7)	6491(4)	17.1(12)
C30	10604(8)	6309(7)	5276(4)	22.4(16)
C15	-1121(9)	1028(8)	9785(5)	28(2)
Zn1B	11584.5(9)	6663.3(8)	2113.6(5)	14.8(2)
Cl1B	12897.7(19)	7214.3(17)	1358.1(10)	21.1(5)
S1B	8408(2)	2794.1(18)	1476.5(10)	19.8(5)
O3B	13995(5)	4067(5)	4816(3)	20.9(13)
O2B	15635(5)	4503(5)	4311(3)	24.1(14)
N1B	10897(6)	5635(5)	1725(3)	16.3(14)
N5B	8515(6)	4144(6)	498(3)	17.1(13)
N4B	10333(6)	6060(5)	2880(3)	13.5(12)
O1B	4755(6)	-183(5)	1024(3)	27.7(14)
N3B	10393(7)	8010(5)	2297(3)	18.6(14)
N2B	12630(6)	6019(5)	2840(3)	14.7(13)
C3B	9670(7)	4408(7)	1274(4)	15.9(14)
C16B	10338(8)	4999(6)	2782(4)	14.4(16)
C4B	10301(8)	5069(7)	879(4)	19.6(16)
C1B	10290(8)	4990(6)	2113(4)	15.7(15)
C17B	10763(7)	6061(6)	3464(4)	13.5(13)
C5B	10887(8)	5667(7)	1117(4)	17.2(15)
C6B	8912(8)	3856(7)	1039(4)	17.3(12)
C2B	9683(8)	4367(7)	1903(4)	16.6(14)
C18B	12075(7)	5791(7)	3410(4)	14.8(12)
C20B	13890(8)	5066(7)	3824(4)	15.7(14)
C25B	9413(8)	7859(7)	2663(4)	15.7(15)
C10B	5981(8)	2189(7)	534(4)	21.9(14)
C21B	14454(8)	5340(7)	3246(4)	18.1(16)
C8B	7569(8)	2771(7)	905(4)	17.7(12)
C23B	14579(8)	4509(7)	4364(4)	17.5(13)
C14B	6897(8)	1134(7)	1393(4)	22.1(17)
C22B	13805(8)	5808(7)	2762(4)	16.7(15)
C9B	6803(8)	2019(7)	945(4)	16.9(14)
C13B	6203(8)	430(8)	1408(5)	25.7(19)
C12B	5375(8)	593(7)	985(4)	20.3(16)
C27B	8838(8)	9680(7)	2733(4)	16.8(15)
C7B	7757(8)	3559(7)	423(4)	20.2(17)
C29B	10591(8)	8976(7)	2124(4)	19.9(17)
C19B	12678(8)	5308(7)	3905(4)	16.4(13)
C30B	8056(8)	10579(7)	3010(4)	21.1(17)
C26B	8615(8)	8680(7)	2898(4)	16.3(15)
C11B	5261(8)	1483(7)	542(4)	23.9(18)
C28B	9832(7)	9823(7)	2335(4)	17.0(15)
C24B	9213(7)	6762(6)	2814(4)	15.7(12)
C15B	3750(9)	31(8)	693(5)	32(2)
O1S	1857(9)	10389(7)	4663(4)	58(2)

N1S	1925(13)	8902(10)	4299(6)	74(3)
C2S	2317(14)	9489(11)	4597(6)	61(3)
C3S	2580(15)	7839(12)	4235(8)	82(4)
C4S	797(17)	9264(15)	4083(10)	108(7)
CaI	13006.3(16)	4466.0(14)	5757.5(8)	17.6(4)
O6W	12390(5)	4873(5)	6773(3)	19.0(12)
O1W	7110(6)	13337(5)	3083(3)	25.0(15)
O2W	2713(7)	11156(5)	5554(3)	37.9(19)
O3W	4735(7)	11855(7)	5001(4)	57(2)
O4W	6582(9)	11989(6)	4096(4)	62(3)
O5W	11832(5)	3248(5)	5667(3)	22.1(13)
O3	3969(6)	12979(5)	6350(3)	28.0(15)
O4B	8257(6)	11461(5)	2790(3)	29.4(15)
O5B	7263(6)	10366(5)	3433(3)	27.8(14)

4. Fluorescence Response Towards Divalent Metal Ions

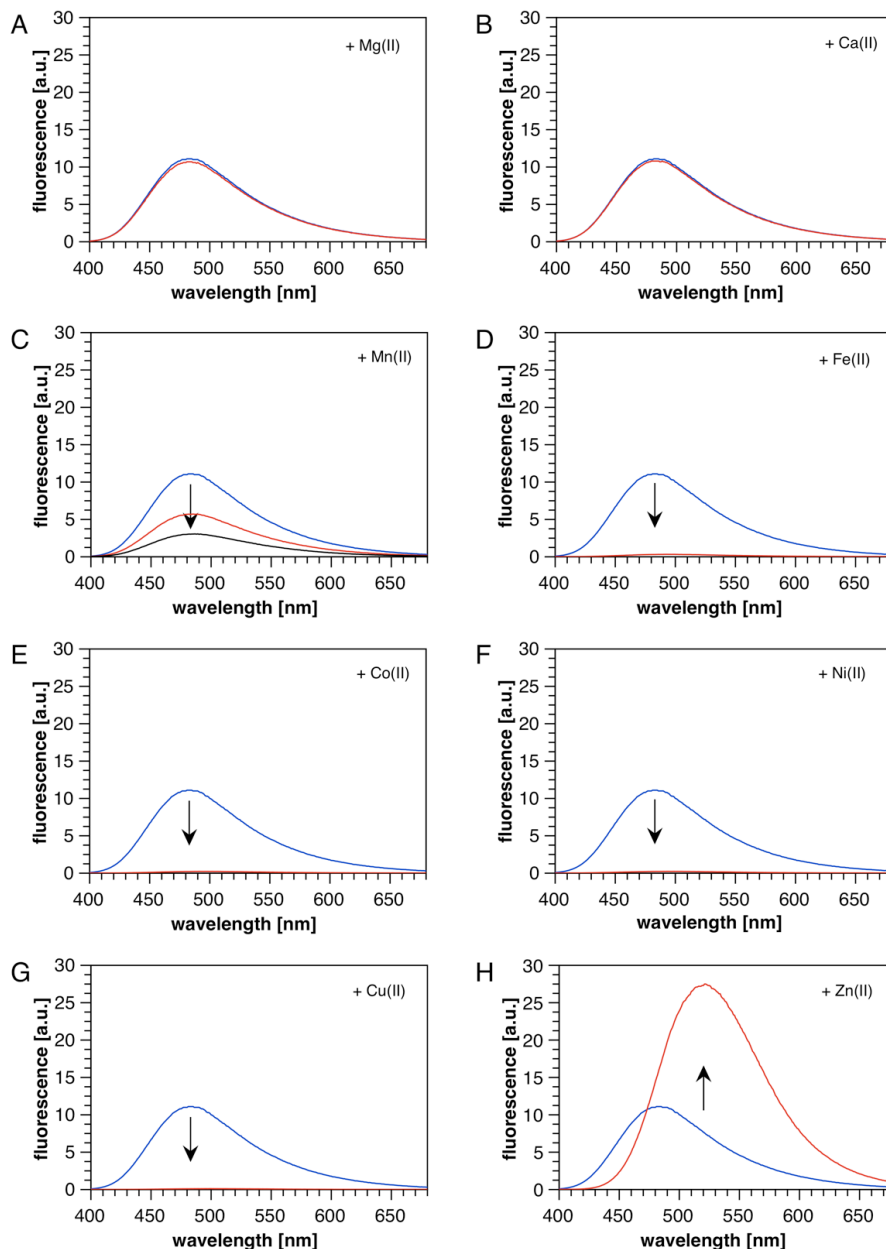
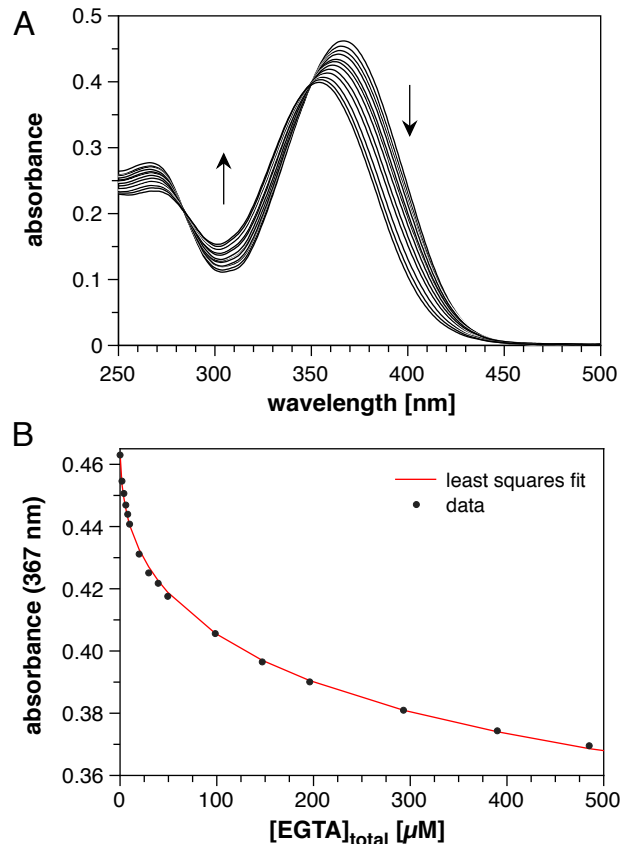


Figure S1: Fluorescence response of chromis-1 acid (**1b**, 5 μM) in the presence of 4.0 equivalents (20 μM) of selected divalent metal ions. A-H) Blue traces represent free chromis-1 acid (5 μM) in pH 7.0 buffer (10 mM PIPES, 0.1 M KCl, 25°C) supplemented with 10 μM EDTA. The red traces were acquired after addition of 20 μM of the corresponding divalent transition metals as indicated. Metal ions were supplied from aqueous stock solutions of the corresponding sulfate salts (Mn(II), Fe(II), Cu(II), and Zn(II)) or nitrate salts (Mg(II), Ca(II), Co(II), and Ni(II)). Black arrows indicate the change in fluorescence after addition of the divalent metals. In plot (C), an additional spectrum (black trace) at a total concentration of 40 μM Mn(II) was acquired. Excitation: 358 nm.

5. Ligand Competition Titrations



Definition of Equilibrium System:

Species	Zn(II)	EGTA	Chromis-1	H	$\log \beta$
Zn(II)	1	0	0	0	0.0
EGTA	0	1	0	0	0.0
Chromis-1	0	0	1	0	0.0
EGTA(H)	0	1	0	1	9.51
EGTA(H ₂)	0	1	0	2	18.25
EGTA(H ₃)	0	1	0	3	21.06
EGTA(Zn(II))	1	1	0	0	12.6
Chromis-1(Zn(II))	1	0	1	0	10.31 ± 0.13

Figure S2: Spectrophotometric determination of the stability constant of chromis-1 acid via competition titration with EGTA. A) Chromis-1 acid (**1b**, 20 μM) was equilibrated with ZnSO₄•7H₂O (20 μM) in aqueous buffer (10 mM PIPES, 0.1 M KCl, pH 7.0, 25°C) treated with Chelex (1% (w/v), Bio-Rad) and titrated with EGTA from 0 to 500 μM. The absorbance spectra were analyzed by non-linear least squares fitting over the spectral range of 250-450 nm to yield an average apparent $\log K_{\text{Zn(II)L}}$ of 10.31 ± 0.13 at pH 7.0 ($n = 8$). B) Change of absorbance at 367 nm and corresponding fit using above equilibrium system definition.

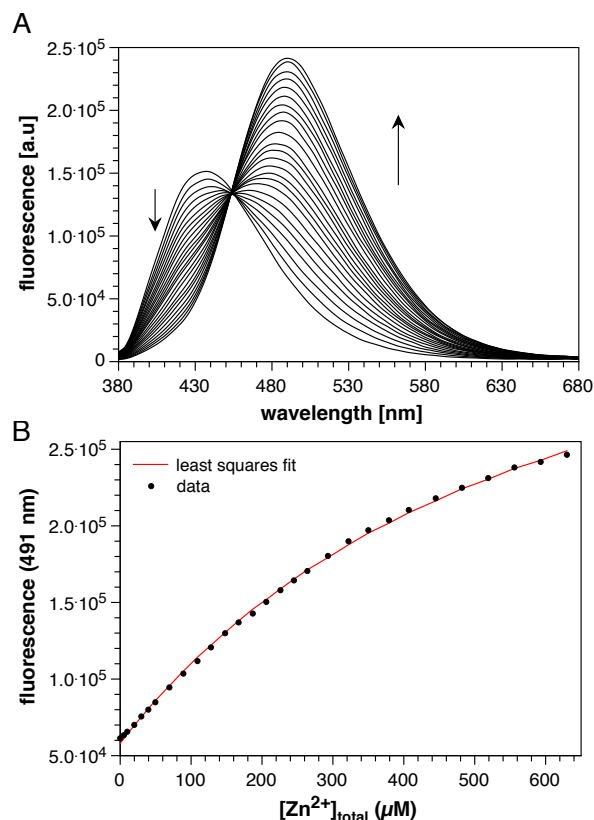


Figure S3: Fluorimetric determination of the stability constant of chromis-1 ester (**1a**) via titration with Zn(II) in the presence of EGTA. A) Chromis-1 ester (**1a**, 2 μM) was equilibrated with EGTA (1 mM) in aqueous buffer (20 mM PIPES, 0.1 M KCl, pH 7.0, 25°C), supplemented with 4:1 DMPC:DMPG liposomes (100 μM), and titrated with $\text{ZnSO}_4 \cdot 7\text{H}_2\text{O}$ to a final Zn(II) concentration 620 μM . Arrows indicate the change in fluorescence after each aliquot of Zn(II) added. The fluorescence spectra (excitation at 358 nm) were analyzed by non-linear least squares fitting over the entire spectral range to give an average apparent $\log K_{\text{Zn(II)L}}$ of 8.62 ± 0.07 ($n = 2$) at pH 7.0. B) Change in fluorescence intensity at 500 nm and corresponding fit using the equilibrium system definition described in Figure S2.

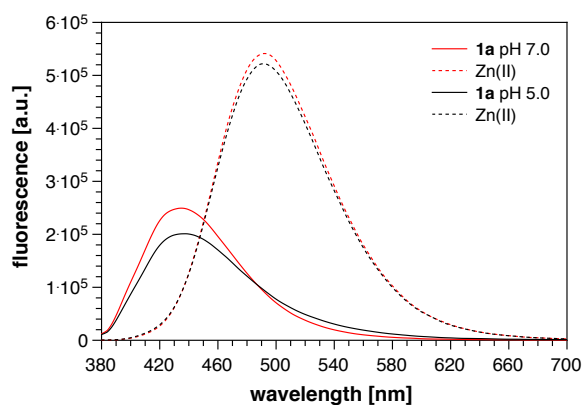
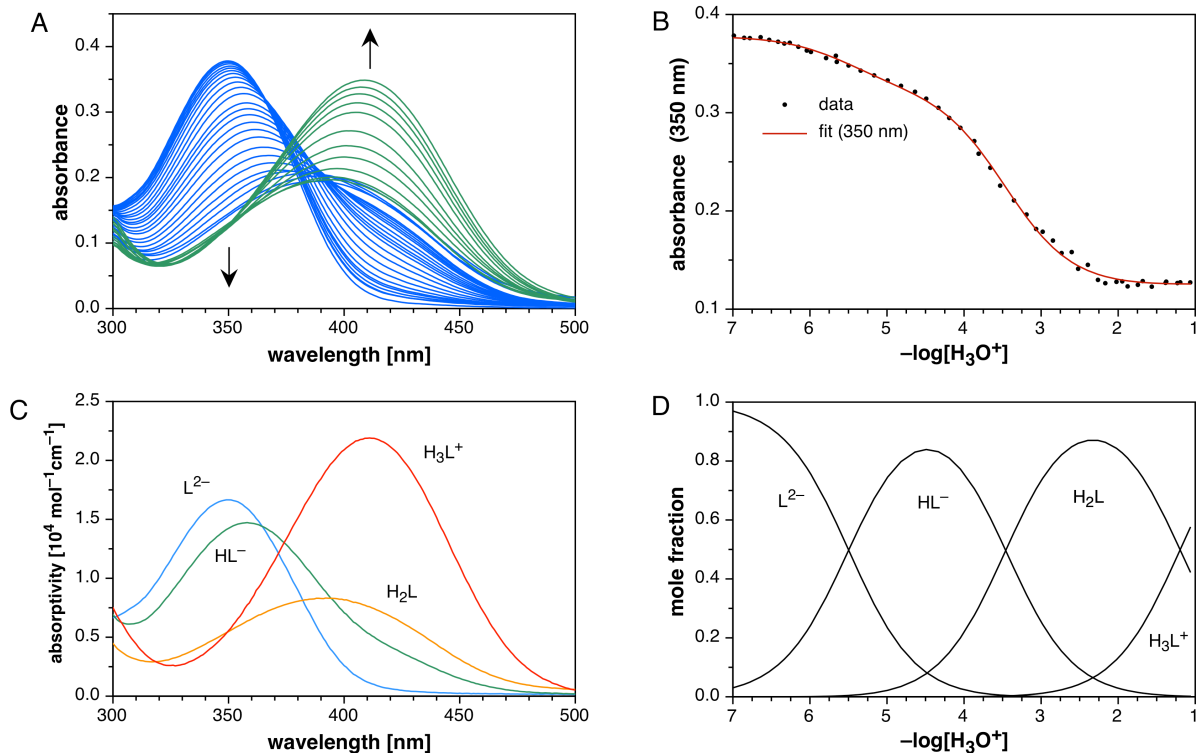


Figure S4. Fluorescence dependence of chromis-1 ester (**1a**) on pH. Chromis-1 ester (2 μM) was equilibrated in aqueous buffer (10 mM PIPES, 100 mM KCl, 25°C) at pH 7.0 and 5.0, both supplemented with 4:1 DMPC:DMPG liposomes (100 μM), and then saturated with $\text{ZnSO}_4 \cdot 7\text{H}_2\text{O}$ (3 μM). Red traces (solid and dashed) represent the fluorescence response of chromis-1 at pH 7.0, and the black traces (solid and dashed) represent the fluorescence response at pH 5.0. Excitation: 358 nm.

6. Spectrophotometric Determination of Protonation Constants



Definition of Equilibrium System:

Species	Chromis-1	H	$\log\beta$
Chromis-1(L)	1	0	0.0
Chromis-1(LH)	1	1	5.49 ± 0.04
Chromis-1(LH ₂)	1	2	8.96 ± 0.05
Chromis-1(LH ₃)	1	3	10.15 ± 0.06

Figure S5: Spectrophotometric determination of the sequential protonation constants of chromis-1 acid (**1b**). A) UV-vis traces upon acidification of a solution of **1b** (22.7 μM) in a mixed PIPES/PIPBS buffer (1 mM, starting pH 7.1, 0.1 M KCl ionic background). The arrows indicate the spectral progression upon acidification. The blue and green traces were acquired in two separate experiments and correspond to the pH ranges of 7.1 to 2.4 and 2.3 to 1.0, respectively. B) Change of absorbance at 350 nm and corresponding fit using above equilibrium system definition. The data were fitted over the entire spectral range from 300-500 nm. The tabulated $\log\beta$ value correspond to sequential protonation constants of $\text{p}K_{\text{a}1} = 5.49$, $\text{p}K_{\text{a}2} = 3.47$, $\text{p}K_{\text{a}3} = 1.19$. C) Deconvoluted spectra for the sequential chromis-1 protonation states. D) Species distribution diagram, calculated based on the experimental $\text{p}K_{\text{a}}$ values.

7. Ratiometric Data Analysis

The ratiometric evaluation of fluorescence imaging data was performed following the original report by Tsien and coworkers.³ For a ratiometric fluorescence probe P with 1:1 Zn(II) binding stoichiometry, the ratio R of the fluorescence intensities at two distinct wavelengths is related to the free metal ion concentration according to equation S1,

$$[\text{Zn(II)}] = K_d \left(\frac{R - R_{\min}}{R_{\max} - R} \right) \left(\frac{S_f}{S_b} \right) \quad (\text{S1})$$

where S_f and S_b are instrument-dependent calibration factors for the free (S_f) and metal-bound (S_b) probe, thus relating the concentration of each species to overall fluorescence intensity F at wavelength λ according to equation S2

$$F(\lambda) = S_f(\lambda)[\text{P}] + S_b(\lambda)[\text{PZn(II)}] \quad (\text{S2})$$

Near $\lambda = 450$ nm, where the emission spectra of the free and Zn(II)-saturated probe cross each other, S_f and S_b are identical and thus the instrument-dependent correction term S_f/S_b assumes unity. Hence, under these conditions the intensity ratio R can be directly related to the free Zn(II) concentration

$$[\text{Zn(II)}] = K_d \left(\frac{R - R_{\min}}{R_{\max} - R} \right) \quad (\text{S3})$$

Furthermore, the fractional saturation of the probe, defined as the ratio of complex concentration $[\text{Zn(II)P}]$ and total probe concentration $[\text{P}]_{\text{total}}$, can also be calculated from the observed intensity ratio R through relationship S4

$$f = \frac{R - R_{\min}}{R_{\max} - R_{\min}} \quad (\text{S4})$$

To validate the applicability of the simplified calibration relationship (S3), Figure S6 illustrates the results from a perfusion experiment with live NIH 3T3 cells, which were exposed to 50 μM ZnSO_4 and 5 μM pyridoxine as described in the main text (Figure 3). Fluorescence micrographs were acquired through two emission band pass filters BP1 (425-462 nm) and BP2 (478-540 nm) at intervals of 20 seconds with two-photon excitation at 720 nm. To calculate the average fluorescence intensity of the individual emission channels for each frame, only pixels with a fluorescence intensity above a threshold of 500, based on 16-bit greyscale resolution, were taken into account. In agreement with the position of the emission cross over point (Figure S3), the averaged fluorescence intensities collected through the shorter wavelength filter (BP1) remained essentially unchanged upon Zn(II) exposure (Figure S6, red circles). Thus, the large increase of the intensity ratio (blue squares) can solely be attributed to the intensity increase of the longer wavelength emission channel (BP2, green circles).

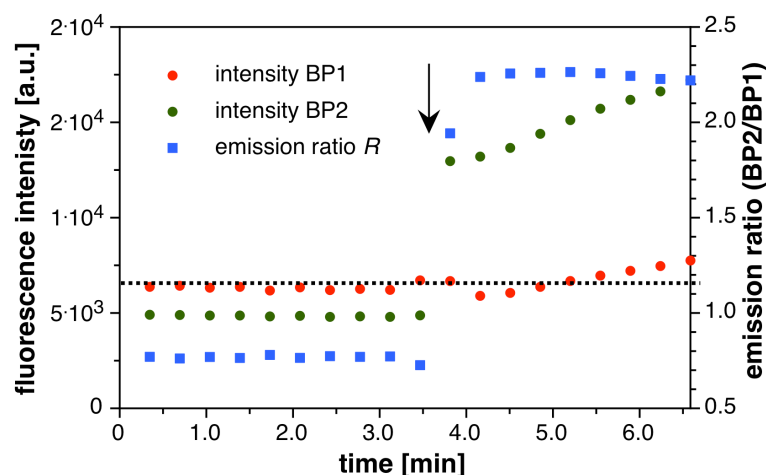


Figure S6. Experimental validation for ratiometric image processing using simplified equation S3. NIH 3T3 cells were incubated with chromis-1 ester (**1a**, 2 μM) and imaged by TPEM with excitation at 720 nm. Fluorescence micrographs were collected through two band pass filters BP1 (425-462 nm) and BP2 (478-540 nm) at 20 second intervals. At the time point indicated with an arrow, 50 μM ZnSO_4 and 5 μM pyrithione were added. While the averaged fluorescence intensity collected through BP1 remained essentially unchanged (red circles), BP2 intensity increased dramatically (green circles) upon Zn(II) exposure, which is also reflected in the emission ratio increase (with $R = \text{BP2/BP1}$).

These data demonstrate that estimates for free Zn(II) concentrations can be directly calculated from the intensity ratio R and the limiting ratios R_{\min} and R_{\max} using the simplified equation S3. For this purpose, the raw fluorescence intensity micrographs of each channel were processed with the quantitative image analysis software package, ImageJ,⁴ using an intensity threshold of 1000 (based on 16-bit greyscale resolution). The resulting ratio images were exported as 32-bit tiff images, and converted to 16-bit color images after applying the corresponding look-up-table (LUT).

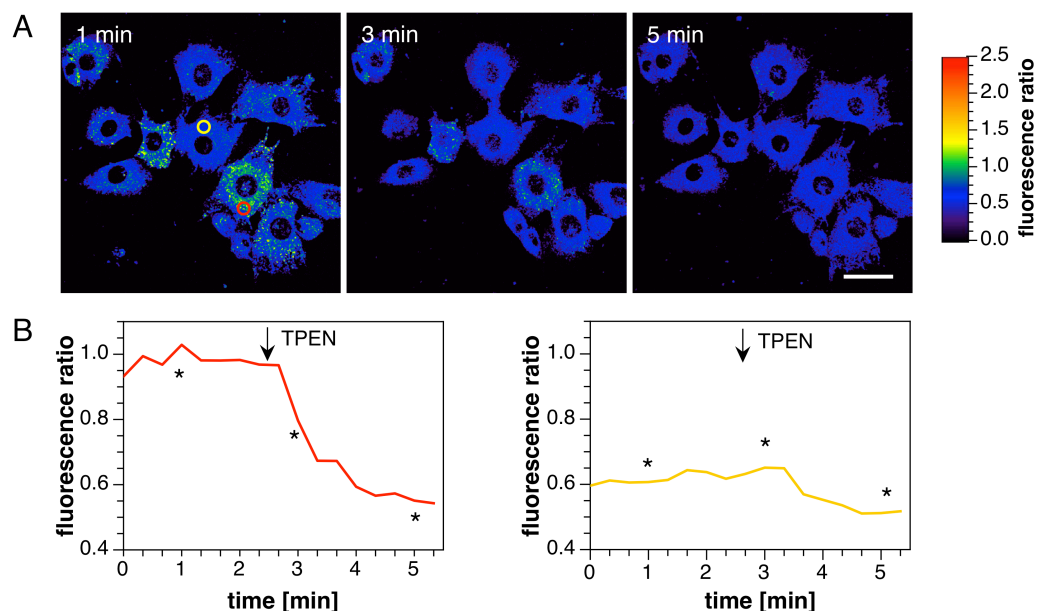


Figure S7. Ratiometric imaging of labile Zn(II) pools in live NIH 3T3 mouse fibroblasts, grown under basal conditions, with chromis-1 ester (**1a**) by TPEN (excitation at 720 nm). (A) Ratio images (BP2/BP1) prior (at 1 min) and after addition (at 3 and 5 min) of 100 μM TPEN (at 2.5 min). Fluorescence intensity images were acquired with two bandpass emission filters BP1 (425-462 nm) and BP2 (478-540 nm) bandpass filters, and the corresponding intensity ratio images were derived based on $R = \text{BP2/BP1}$. The false-color ratio scale (LUT) is shown to the right. Scale bar: 40 μm . (B) Time course of the average intensity ratio change for the ROIs indicated with a yellow and red circle, respectively, in panel (A). The asterisks indicate the respective time points of the ratio images depicted in panel (A).

8. References:

1. Sumalekshmy, S.; Henary, M. M.; Siegel, N.; Lawson, P. V.; Wu, Y.; Schmidt, K.; Brédas, J. L.; Perry, J. W.; Fahrni, C. J., Design of Emission Ratiometric Metal-Ion Sensors with Enhanced Two-Photon Cross Section and Brightness. *J. Am. Chem. Soc.* **2007**, *129* (39), 11888-11889.
2. Kojima, T.; Hayashi, K. I.; Iizuka, S. Y.; Tani, F.; Naruta, Y.; Kawano, M.; Ohashi, Y.; Hirai, Y.; Ohkubold, K.; Matsuda, Y.; Fukuzumi, S., Synthesis and characterization of mononuclear Ruthenium(III)Pyridylamine complexes and mechanistic insights into their catalytic alkane functionalization with m-chloroperbenzoic acid. *Chem. Eur. J.* **2007**, *13* (29), 8212-8222.
3. Grynkiewicz, G.; Poenie, M.; Tsien, R. Y., A New Generation of Ca^{2+} Indicators with Greatly Improved Fluorescence Properties. *J. Biol. Chem.* **1985**, *260* (6), 3440-3450.
4. Schneider, C. A.; Rasband, W. S.; Eliceiri, K. W., NIH Image to ImageJ: 25 years of image analysis. *Nat. Methods* **2012**, *9* (7), 671-675.